Optimal Configuration of Hydrogen-Embrittlement-Fabricated Nanogaps for Surface-Conduction Electron-Emitter Display

Yiming Li, *Member, IEEE*, and Hui-Wen Cheng, *Student Member, IEEE*

***Abstract*—Application of nanogaps for electron sources is fascinating in surface-conduction electron-emitter display. In contrast to rather complicated fabrication processes of the focused ion beam technique for the extremely narrow fissure, nanogaps fabricated by hydrogen embrittlement (HE) have thus been proposed as novel surface-conduction electron emitters due to their low turn-ON voltage, high emission current, high focus capability, and high emission efficiency. In this paper, we theoretically investigate effects of the separation width and the tilted angle of the nanogaps fabricated by HE method on the field emission efficiency using a 3-D finite-difference time-domain particle-in-cell simulation technique. The structure with a large tilted angle may result in a high emitted current, but the collected current on the anode is suppressed due to the strong local field around the tip. A small structure prevents the emitted electrons from spreading out, and thus, no current could be collected by the anode. Also, the structure with a wide (or a narrow) separation of gap weakens (or enhances) the field around the tip and reduces the collected electrons. For better emission efficiency and focus capability, the separation width and the tilted angle of the examined structure could vary from 57 to 117 nm and 30° to 60°, respectively.**

***Index Terms*—Collected electron current, emitted electron current, field emission efficiency, focus capability, Fowler–Nordheim equation, finite-difference time-domain (FDTD) particle in cell (PIC), hydrogen embrittlement, Maxwell's equations, motion trajectory, nanogaps, palladium, separation width, surface conduction electron emitters, tilted angle.**

I. Introduction

SURFACE-CONDUCTION electron-emitter display (SED) based upon surface-conduction electron emitters (SCEs) [1]–[6] is one of new type flat panel displays. Our recent investigations have indicated that the technique involving field emission properties of novel SCEs with nanogaps fabricated by hydrogen embrittlement (HE) as field emission sources is superior to the conventional focused ion beam (FIB) technique [7]–[11]. It is known that the geometrical configuration of the nanogaps fabricated by HE method may have significant influence on the field emission of SCEs. However, the study on optimal configuration, such as the separation width and the tilted angle of the novel nanogaps fabricated by HE method, has not been reported to date.

To obtain better field emission property and a higher focus capability for advanced SED applications, we study the effect of the separation width and the tilted angle of cathodes on the emission efficiency of SCEs with the nanogaps fabricated by HE method. A 3-D particle-in-cell (PIC) method, coupled with the finite-difference time-domain (FDTD) scheme, is adopted to explore the optimal configuration of the novel nanogaps on the palladium (Pd) thin-film strip. However, to obtain the desired field emission properties, the designing variables are modified. The 3-D FDTD-PIC scheme includes the space charge effects automatically, which allows us to analyze the final steady-state effect of configuration on the conducting mechanism and the field emission efficiency of the Pd hydrogenation nanogap field emission emitter. The result obtained in this study shows that the nanogap fabricated by HE method on the Pd thin-film strip with a large tilted angle may result in high emitted currents, but the collected current on the anode is suppressed due to the strong local field around the tip of the nanogap. For the novel SCE with a small angle, the structure prevents the emitted electrons from spreading out, and thus, no current could be collected by the anode. In addition, the novel SCE with wide separation of gap weakens the field around the tip. Similarly, we have an enhanced local field around the tip for the structure with a narrow separation of gap. Both of them will reduce the collected electrons. According to our preliminary examinations, we thus find a tradeoff between the tilted angle and the separation width of the nanogap fabricated by HE method. For better emission efficiency and high focus capability, the gap width could range from 57 to 117 nm and the tilted angle could vary from 30° to 60°.

This paper is organized as follows. Section II describes the nanogaps fabricated by HE method for the SCE structure and the simulation procedure. In Section III, the emission current, the electronic trajectories, the electric field distribution near the nanogaps, and the emission efficiency are examined with respect to different tilted angle and separation width of gap. Finally, conclusions are drawn.

II. Structure and Simulation Technique

For the structure of SCE to be explored, a 150-nm-thick SiO_2 layer was first thermally grown on the Si substrate. The Ti layer

Manuscript received January 3, 2009. First published June 10, 2009; current version published November 11, 2009. This work was supported in part by Taiwan National Science Council (NSC) under Contract NSC-97-2221-E-009-154-MY2. The review of this paper was arranged by Associate Editor H. Misawa.

Y. Li is with the Department of Electrical Engineering, National Chiao Tung University, Hsinchu 300, Taiwan, and also with the National Nano Device Laboratories, Hsinchu 300, Taiwan (e-mail: ymli@faculty.nctu.edu.tw).

H.-W. Cheng is with the Institute of Communication Engineering, National Chiao Tung University, Hsinchu 300, Taiwan (e-mail: hwcheng@mail.ymlab.org).

Color versions of one or more of the figures in this paper are available online at http://ieeexplore.ieee.org.

Digital Object Identifier 10.1109/TNANO.2009.2024535

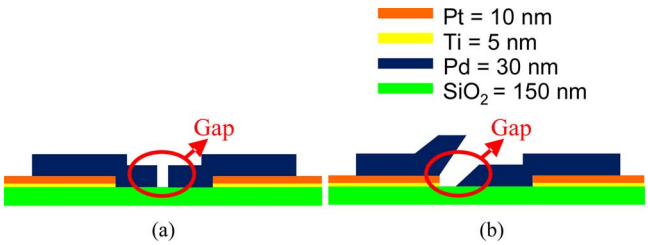

Fig. 1. Cross-sectional illustration of the (a) FIB and (b) nanogaps fabricated by HE method within the structure of SCEs.

with 5 nm thickness was electron beam (e-beam) evaporation deposited on the oxide as an adhesion layer for the subsequently deposited Pt thin film with a thickness of 10 nm. The pattering of the Pt/Ti line electrodes with a width of 80 μm was photolithographically performed using a liftoff method. The 30-nm-thick Pd thin film [12]–[14] is deposited on the Pt/Ti bottom electrode, and liftoff method is also used to pattern the 50-μm-long and 3-μm-wide Pd electrode line [15]–[17], where the material settings are shown in the upper right of Fig. 1. Electron emission characteristics in the nanogaps are studied using a dc voltage power supply. The measurement is carried out under a vacuum condition of 10^{-6} torr [18], [19]. We notice that the shape of nanogap could be controlled by two different treatments. Gaps with a right vertical angle could be formed by the focused ion beam (FIB) energy [20]–[22], and the gaps with various tilted angles are fabricated by the high-pressure hydrogen absorption treatment, as shown in Fig. 1(a) and (b), respectively [23], [24]. Details of fabrication characterization and calibration of the conventional and novel structures have been reported in our previous works [7]–[11].

To explore the effect of the tilted angle and the separation width on the emission efficiency and focus capability of the nanogap fabricated by HE method on the Pd thin-film of the SCE, starting from a specified initial state, according to [25], we solve Maxwell's equation

$$\begin{cases} \dfrac{\partial \vec{B}}{\partial t} = -\vec{\nabla} \times \vec{E} \\ \dfrac{\partial \vec{E}}{\partial t} = -\dfrac{\vec{J}}{\varepsilon} + (\mu\varepsilon)^{-1} \vec{\nabla} \times \vec{B} \\ \vec{\nabla} \cdot \vec{E} = \dfrac{\rho}{\varepsilon} \\ \vec{\nabla} \cdot \vec{B} = 0 \end{cases} \tag{1}$$

and then obtain Lorentz's force

$$\begin{cases} \vec{F} = q(\vec{E} + \vec{v} \times \vec{B}) \\ \dfrac{\partial \vec{x}}{\partial t} = \vec{v}. \end{cases} \tag{2}$$

We notice that $\vec{E}$ and $\vec{B}$ are the vectors of electric and magnetic fields, respectively, $\vec{x}$ and $\vec{v}$ the vectors of position and velocity of electron, respectively, ε and μ are permeability and permittivity, and $\vec{J}$ and ρ are the current density vector and charge density resulting from charge particles, respectively. For each PIC procedure, the fundamentals of PIC are briefly described [26]–[28]; the full set of 3-D Maxwell's equations is simultaneously solved using FDTD method to obtain electromagnetic fields [26]–[30]. The electrons are moved according to the fields advanced in each time step. The obtained electron density and current density are successively used as sources for advancing the electromagnetic fields. This 3-D FDTD-PIC method forms a self-consistent simulation of the electromagnetic fields and charged particles, as shown in Fig. 2 [10]. These steps are repeated for each time step until the specified number of time steps is reached.

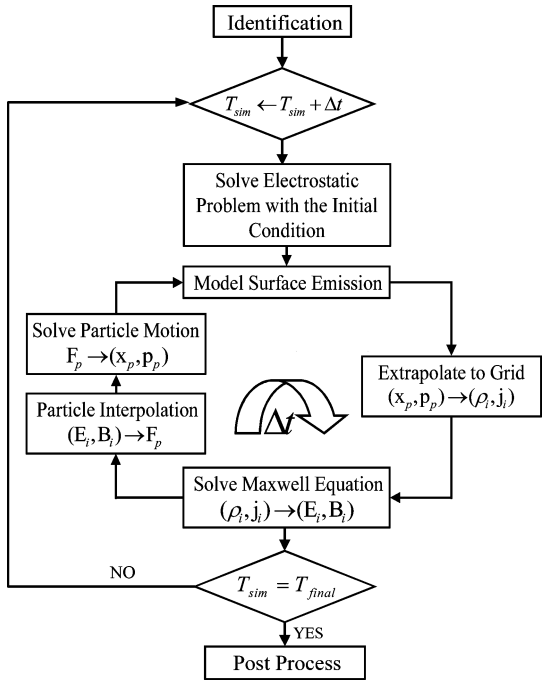

Fig. 2. Computational scheme for field emission simulation.

In the field emission process, the electron emission is calculated by the Fowler–Nordheim equation [31]

$$J = \frac{AE^2}{\varphi t^2} \exp\left(\frac{-Bv(y)\varphi^{3/2}}{E_{\mathrm{N}}}\right) \tag{3}$$

where the experimentally validated coefficients A and B are 1.541×10^{-6} A·eV/V^2 and 6.3408×10^8 eV$^{-3/2}$·V·μm^{-1}, E_{N} is the normal component of the electric field at the emitter surface, φ is the work function of the emission material [32]–[35], $t^2 = 1.1$, and $v(y) = 0.95 - y^2$, with $y = 3.79 \times 10^{-5} \times E^{1/2}/\varphi$ being in SI unit [7]–[11].

We have previously observed that the SCEs fabricated by HE method have a higher focus capability than that of the conventional one fabricated by FIB method [7], [10]. To pursue the higher field emission efficiency and more focus capability, we further examine the geometrical configuration of the structure fabricated by HE method and the property of its field emission. Section III simultaneously optimizes the tilted angle, ranging from 10° to 80°, and the gap width, varying from 0 to 147 nm, of Pd (morphology of the emitters) to investigate the characteristics of field emission.

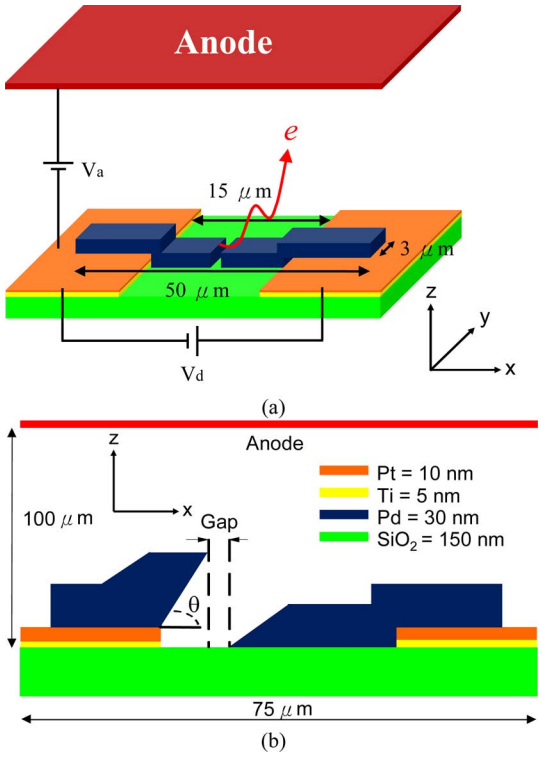

Fig. 3. (a) Schematic plot of the SED structure, where the SCE is fabricated by high-pressure hydrogen absorption treatment, where $V_a + V_d = 2000$ V and $V_d = 40$ V. (b) Cross-sectional plot of the SCE along the x–z plane, where the gap and θ are the separation width and the tilted angle.

III. Results

Fig. 3(a) and (b) illustrates the overview of the SED structure and the cross-sectional plot of nanogaps fabricated by HE method on the x–z plane. The anode voltage (V_a) and cathode voltage (V_d) are fixed at 1960 and 40 V for all of the following calculations. We notice that the SCEs fabricated by HE method under such bias condition maintain enough voltage to turn on the emitter electrode based on our experimental characterization [7]–[11]. The gap width and the tilted angle of SED, as shown in Fig. 3(b), are two process variables to be examined for designing a high-performance SED device. We first find that the SED collects no current on the anode electrode if the separation width and the tilted angle of SCE nanogap are 147 nm and 10°. The structure with an extremely tilted angle weakens the strength of electric field around the emitter, as shown in Fig. 4(a); from the electronic trajectory perspective, which is shown in Fig. 4(b), the emitted electrons under this configuration are strongly blocked by the geometry.

For the case with a smaller separation width and a larger tilted angle, 0 nm and 80°, for example, a large number of electrons are emitted from the emitters due to a strong electric field, as shown in Fig. 5(a). The narrower gap width implies the stronger electric field. The electric field between the left and right emitter electrodes is strong enough to attract more electrons due to smaller gap width, as shown in Fig. 5(b).

However, more emitted electrons are attracted, and hence, move downward along the direction of the strong electric field

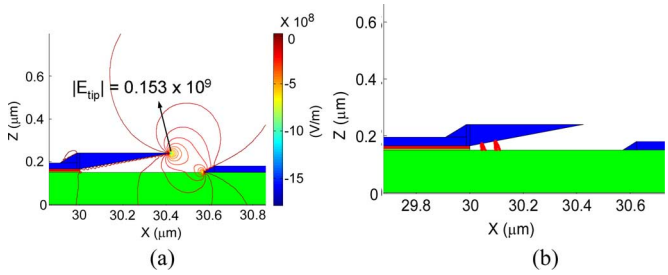

Fig. 4. Plot of (a) electric field and (b) electronic trajectory. Both of them result from the structure with 147 nm separation width and 10° tilted angle.

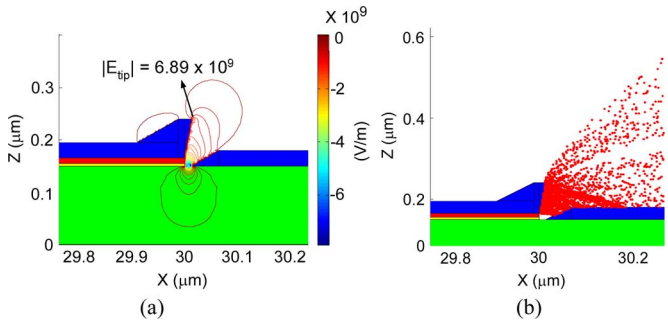

Fig. 5. Plot of (a) electric field and (b) electronic trajectory for the structure with 0 nm separation width and 80° tilted angle.

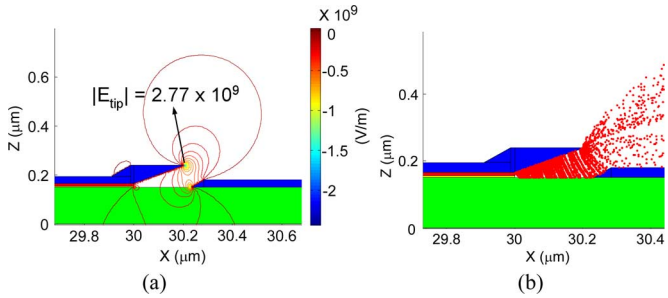

Fig. 6. Plot of (a) electric field and (b) electronic trajectory for the structure with 27 nm separation width and 20° tilted angle.

around the tip of electric field. It results in more electrons being absorbed by the cathodes because the distribution of electric filed is limited in a smaller region. Only very few emitted electrons could be collected by the anode. According to the earlier observations, we know that too narrow separation width or large tilted angle will decrease the collected current due to a strong electric field around the apex of cathodes. The most part of emitted electrons moves downward rapidly; consequently, the anode electrode could merely collect few electrons.

For example, if we further decrease the tilted angle from 80° to 20° and increase the separation width of gap from 0 to 27 nm, the strength of electric field is reduced and the distribution of electric field becomes wider, as shown in Fig. 6(a). Compared with the SCE with 0 nm separation width and 80° tilted angle, the electric field reduction is about 60% due to a wider gap. However, the gap width is still narrow that could not prevent the emitted electrons from moving downward to be absorbed, as shown in Fig. 6(b). Only fewer emitted electrons are attracted

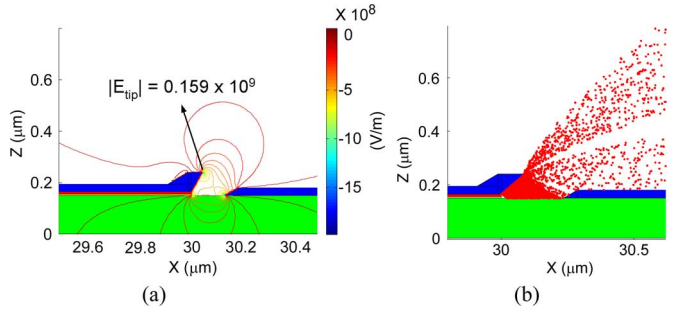

Fig. 7. Plot of (a) electric field and (b) electronic trajectory for the structure with 87 nm separation width and 40° tilted angle.

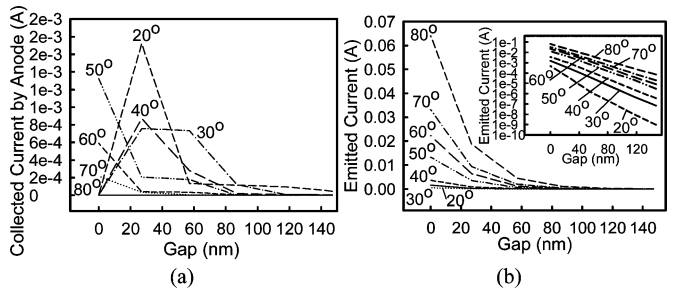

Fig. 8. Plot of (a) collected and (b) emitted currents for the separation width from 0 to 147 nm and the tilted angle from 10° to 80°. The inset of (b) is the emitted current in the log scale.

by the tip of electrode due to the weak electric field. Most of electrons are moving upward as they are attracted by the anode, and thus, result in large collected current, and a high efficiency of field emission could be expected. We know that an increased tilted angle can avoid significant reduction of the strength of electric field. For a wide gap width, only few electrons could be emitted from the electrode due to the weaker electric field. As the gap width is increased from 27 to 87 nm and the tilted angle is slightly increased from 20° to 40°, the gap with the larger titled angle demonstrates that the distribution of electric field is wider and extends upward from the electrode, as shown in Fig. 7(a). Thus, more emitted electrons move upward. Compared with the case of 0 nm and 80°, the electric field reduction is about 45%. The reduction of electric field is less than that for the case of 27 nm and 20°. We could conclude that the variation of titled angel is more sensitive than the variation of gap width in field emission. It is found that more emitted electrons move upward to the anode as the driving voltage is increased, as shown in Fig. 7(b). Consequently, there is a tradeoff between the separation width of gap and the tilted angle. According to the analyses given before, the collected and emitted currents are shown with respect to different separation width and tilted angle of SCE nanogap in Fig. 8(a) and (b), respectively. By defining the efficiency as the collected current divided by the emitted current and considering the emitted current, which is greater than 1×10^{-6} A, as a criterion for the following efficiency calculation, the estimated efficiency is shown in Fig. 9, where the electric field, emitted and collected currents, and efficiency for the interesting cases of 57 and 117 nm are listed in Table I. Most of emitted electrons enter into the oxide conduction band,

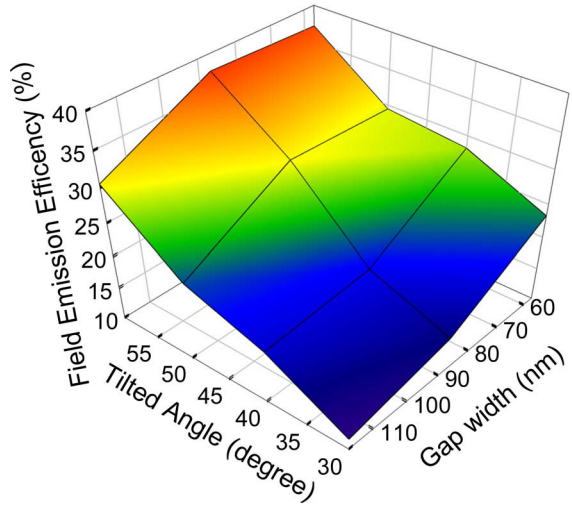

Fig. 9. Efficiency versus the separation width and the tilted angle for the investigated SED.

TABLE I
ELECTRIC FIELD, EMITTED CURRENT, COLLECTED CURRENT, AND EFFICIENCY FOR 57 nm GAP AND 117 nm GAP WITH TILTED ANGLES 30° AND 60°, RESPECTIVELY

	57 nm		117 nm	
	30°	60°	30°	60°
Electric field (V/m)	4.3×10^{9}	5.7×10^{9}	1.6×10^{9}	2.4×10^{9}
Emitted Current (A)	8.66×10^{-4}	9.33×10^{-3}	2.29×10^{-6}	8.56×10^{-5}
Collected Current (A)	3.47×10^{-5}	7.34×10^{-4}	4.13×10^{-7}	9.97×10^{-6}
Efficiency (%)	23.28	37.22	11.64	30.50

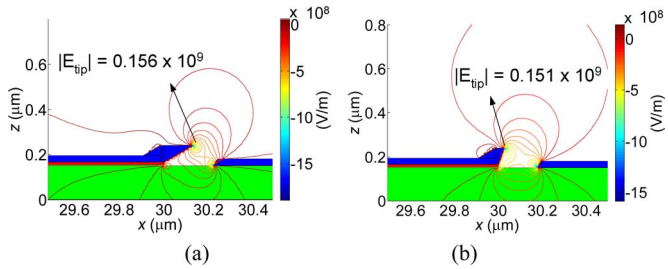

Fig. 10. Plot of the electric field for the case of structure with (a) 87 nm gap and 30° tilted angle and (b) 147 nm gap and 80° tilted angle.

which results in degradation of efficiency. It is then noted that the gap width and the tilted angle have an influence on the amount of electrons that enter the oxide. The results show that the explored structure with the range of the separation width from 57 to 117 nm and the larger tilted angle from 30° to 60° possess promising emission efficiency.

To investigate the focus capability, we further examine the SCE structure with 80° tilted angle and 147 nm gap, which is out of the suggested range. We compare it with the SCE with 30° tilted angle and 87 nm gap, where they have similar strength of electric fields, as shown in Fig. 10(a) and (b). The distribution of electric field for the case with 30° tilted angle and 87 nm gap is relatively small, and the emitted electrons can move upward

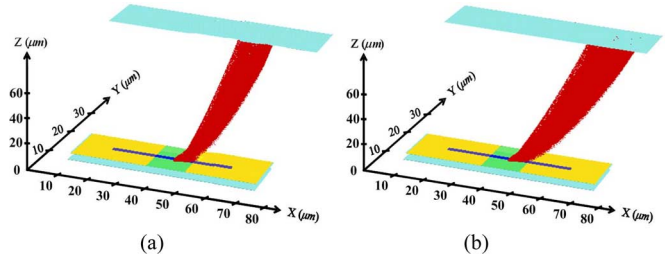

Fig. 11. 3-D electronic trajectories of the cases with (a) 87 nm gap and 30° tilted angle and (b) 147 nm gap and 80° tilted angle.

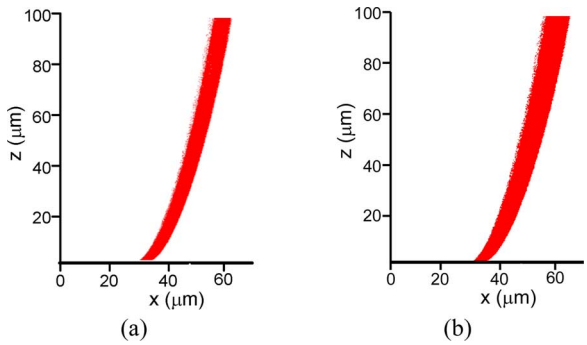

Fig. 12. Plot of the electronic trajectories on the x–z plane of the cases with (a) 87 nm gap and 30° tilted angle and (b) 147 nm gap and 80° tilted angle.

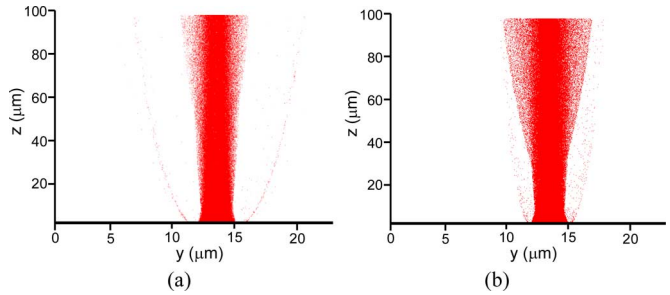

Fig. 13. Plot of the electronic trajectories on the y–z plane of the cases with (a) 87 nm gap and 30° tilted angle and (b) 147 nm gap and 80° tilted angle.

and are localized centrally. However, the emitted electrons with a wider gap width spread out. The corresponding 3-D electronic trajectories are shown in Fig. 11(a) and (b). On the x–z plane, the electronic trajectory of the SCE with 147 nm gap and 80° tilted angle is wider than that of the case with 87 nm gap and 30° tilted angle, as shown in Fig. 12(a) and (b); on the y–z plane, it is obvious that the SCE structure with 87 nm gap and 30° tilted angle has higher focus capability than the other one, as shown in Fig. 13(a) and (b), respectively. From a view of current density distribution on the anode, the SCE with 87 nm gap and 30° tilted angle has a higher collected current and focus capability than that of the SCE with 147 nm gap and 80° tilted angle, as shown in Fig. 14(a) and (b). Compared to the SCE with 87 nm gap and 30° tilted angle, the strength of electric field in the SCE with 147 nm gap and 80° tilted angle is reduced by 17% and collected current is reduced by 80.4%. SCEs with a larger tilted angle have a stronger electric field, but more emitted electrons will move downward against the anode. Thus, the collected current

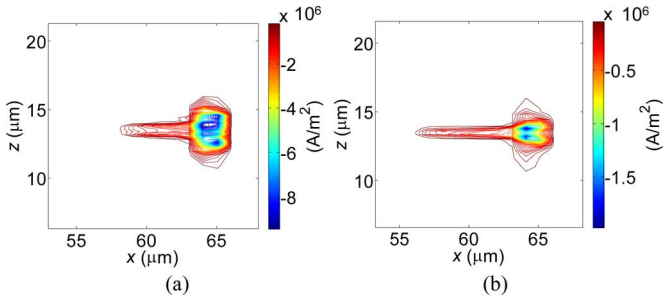

Fig. 14. Current density distribution on the anode for the case of structure with (a) 87 nm gap and 30° tilted angle and (b) 147 nm gap and 80° tilted angle.

TABLE II
LOSS (IN PERCENT) OF EMITTED CURRENT ENTERING IN THE OXIDE UNDER DIFFERENT GEOMETRY DESIGNS

SCEs	Loss of I_e (%)
147 nm separation width and 10° tilted angle	97%
0 nm separation width and 80° tilted angle	87%
27 nm separation width and 20° tilted angle	83%
87 nm separation width and 40° tilted angle	78%

will be reduced. We know that the SCE with a wider gap width absorbs fewer electrons from electrode due to the weak electric field. Therefore, for better field emission efficiency and higher focus capability, the separation width of gap varying from 57 to 117 nm and the tilted angle within 30°–60° are suggested.

IV. DISCUSSIONS

The current conservation law tells us that the total emitted current at the left electrode (I_e) is the sum of the current at the right electrode (I_d), the current flowing to the substrate oxide (I_{ox}), and the current collected by the anode (I_a). The substrate oxide may be heated by I_{ox}, because the entered electrons have energies higher than the oxide conduction band edge. However, since the mechanism of how the emission rate is affected is unknown, we ignore the influence of these trajectories in the present simulation. Taking into consideration the discrepancy $I_e - (I_d + I_a)$, the efficiency turned out to be less than 50%, i.e., we have more than 50% loss of emitted electrons due to the trajectories. As shown in Fig. 4(a), since the electric flux distribution of SCEs with 147 nm separation width and 10° tilted angle spreads widely and deeply into the oxide, most of the emitted electrons must enter the oxide conduction band along the electric flux lines. The efficiency turned out to be degraded by 97% due to I_{ox}. As shown in Fig. 5(b), since the gap width is too narrow for the emitted electrons to enter into the oxide, this suppresses the degradation of efficiency, which results in 87% loss of I_e. As shown in Fig. 6(a), the SCEs with 27 nm separation width and 20° tilted angle reduce the electric field, whereas the wider gap width results in wider distribution of electric field into the oxide. We still have the 83% loss of I_e. As shown in Fig. 7(a), the SCE with 87 nm separation width and 40° tilted angle exhibits larger electric field, and more electrons are emitted due to larger tilted angle. For more emitted current, the amounts of both I_{ox} and I_a increase. Consequently, there is a tradeoff between gap width and tilted angle, where the variation

of I_{ox} depends on the gap width and tilted angle, as indicated in Table II.

V. Conclusion

In this study, a single nanogap in the Pd strip electrode of a novel SCE structure by hydrogen absorption under high-pressure treatment has been explored, where the field emission efficiency has been optimized by varying the separation width of gap and the tilted angle. The emitter with a small tilted angle limits those emitted electrons to move upward to the anode and reduces the collected current. Therefore, a fixed separation width of gap with a higher tilted angle has been examined. The high electric field gathered around the emitter tip induces a higher emission current. However, the high electric field around the emitter tip attracts more emitted electrons and reduces the collected current on the anode. On the other hand, a wide gap between two electrodes of cathode decreases the electric field and reduces the number of emitted electrons. Thus, a narrow space between two electrodes has been used to increase the electric field and emit a large number of electrons. The stronger electric field between two electrodes attracts electrons and reduces the collected current. For better field emission efficiency, the separation width of gap could be varied from 57 to 117 nm, and the range of tilted angle is within 30°–60° for the SED under the specified bias condition. We are currently studying the field emission property of the novel nanogap fabricated by HE method with different material and morphology. Such investigation may produce higher emission current under lower supply voltage, and thus, it will benefit high-performance SED application. With regard to the current entering the oxide, we will study it in our future work.

Acknowledgment

The authors express their appreciation to the referee for an exceptional in-depth reading of the paper.

References

[1] M. A. Reed, C. Zhou, C. J. Muller, T. P. Burgin, and J. M. Tour, "Conductance of a molecular junction," *Science*, vol. 278, no. 5336, pp. 252–254, 1997.

[2] W. Liang, M. P. Shores, M. Bockrath, J. R. Long, and H. Park, "Kondo resonance in a single-molecule transistor," *Nature*, vol. 417, pp. 725–729, 2002.

[3] C. H. Tsai, F. M. Pan, K. J. Chen, C. Y. Wei, M. Liu, and C. N. Mo, "Nanogap formation by palladium hydrogenation for surface conduction electron emitters fabrication," *Appl. Phys. Lett.*, vol. 90, pp. 163115–163117, 2007.

[4] I. Nomura, K. Sakai, E. Yamaguchi, M. Yamanobe, S. Ikeda, T. Hara, K. Hatanaka, and Y. Osada, "A new emissive display based on surface-conduction electron-emitters," in *Proc. IDW*, 1996, pp. 523–526.

[5] K. Sakai, I. Nomura, E. Yamaguchi, M. Yamanobe, S. Ikeda, T. Hara, K. Hatanaka, Y. Osada, H. Yamamoto, and T. Nakagiri, "Flat-panel displays based on surface-conduction electron-emitters," in *Proc. EuroDisplay*, 1996, pp. 569–572.

[6] E. Yamaguchi, K. Sakai, I. Nomura, T. Ono, M. Yamanobe, N. Abe, T. Hara, K. Hatanaka, Y. Osada, H. Yamamoto, and T. Nakagiri, "A 10-in. surface-conduction electron-emitter display," *J. Soc. Inf. Display*, vol. 5, no. 4, pp. 345–348, 1997.

[7] Y. Li and H. Y. Lo, "Surface conduction electron emission in palladium hydrogenation nanogaps," *Phys. D, Appl. Phys.*, vol. 41, pp. 085301-1–085301-6, 2008.

[8] H. Y. Lo, Y. Li, H. Y. Chao, C. H. Tsai, and F. M. Pan, "Field-emission properties of novel palladium nanogaps for surface conduction electron-emitters," *Nanotechnology*, vol. 18, pp. 475708-1–475708-7, 2007.

[9] H. Y. Lo, Y. Li, C. H. Tsai, H. Y. Chao, and F. M. Pan, "Effect of process variation on field emission characteristics in surface conduction electron-emitters," *IEEE Trans. Nanotechnol.*, vol. 7, no. 4, pp. 434–439, Jul. 2008.

[10] Y. Li, H.-Y. Chao, and H.-Y. Lo, "High field emission efficiency surface conduction electron emitters," *J. Comput. Electron.*, vol. 7, pp. 440–444, 2008.

[11] C.-H. Tsai, K.-J. Chen, F.-M. Pan, H.-Y. Lo, Y. Li, M.-C. Chiang, and C.-N. Mo, "Effects of hydrogen plasma treatment on field-emission characteristics of palladium nanogap emitters," *J. Electrochem. Soc.*, vol. 155, pp. 361–364, 2008.

[12] F. A. Lewis, *The Palladium/Hydrogen System*. London, U.K.: Academic, 1967.

[13] E. Wicke and H. Brodowsky, "Hydrogen in palladium and palladium alloys," in *Hydrogen in Metals II, Application-Oriented Properties, Topics in Applied Physics,* vol. 29, G. Alefeld and J. Völkl, Eds. Berlin, Germany: Springer-Verlag, 1978, p. 73.

[14] W. Zhong, Y. Cai, and D. Tomanek, "Mechanical stability of Pd–H systems: A molecular dynamics study," *Phys. Rev. B*, vol. 46, pp. 8099–8109, 1992.

[15] M. Aoyagi, "Temperature characteristics of stress-induced migration based on atom migration," *J. Vac. Sci. Technol. B*, vol. 23, pp. 2384–2389, 2005.

[16] C. J. Zhai and R. C. Blish, "A physically based lifetime model for stress-induced voiding in interconnects," *J. Appl. Phys.*, vol. 97, pp. 113503–113508, 2005.

[17] M. Aoyagi, "Temperature characteristics of stress-induced migration based on atom migration," *J. Vac. Sci. Technol. B*, vol. 23, pp. 2384–2389, 2005.

[18] W. Zhu, P. K. Baumann, and C. A. Bower, *Vacuum Microelectronics*. New York: Wiley, 2001.

[19] I. Brodie and P. R. Schwoebel, "Vacuum microelectronic devices," *Proc. IEEE*, vol. 82, no. 7, pp. 1006–1018, Jul. 1994.

[20] Y. Goth, T. Ohtake, N. Fujita, K. Inoue, H. Tsuji, and J. Ishikawa, "Fabrication of lateral-type thin-film edge field emitters by focus ion beam technique," *J. Vac. Sci. Technol. B*, vol. 13, no. 2, pp. 465–468, 1995.

[21] H. Fujii, S. Kanemaru, H. Hiroshima, S. M. Gorwadkar, T. Matsukawa, and J. Itoh, "Fabrication and characterization of a nanogap edge emitter with a silicon-on-insulator wafer," *Appl. Surf. Sci.*, vol. 146, no. 1, pp. 203–208, 1999.

[22] K. Shigeto, M. Kawamura, A. Yu. Kasumov, K. Tsukagoshi, K. Kono, and Y. Aoyagi, "Reproducible formation of nanoscale-gap electrodes for single-molecule measurements by combination of FIB deposition and tunneling current detection," *Microelectron. Eng.*, vol. 83, no. 4, pp. 1471–1473, 2006.

[23] G. Mulas, F. Delogu, C. Pistidda1, and G. Cocco, "Mechanochemical effects on hydrogen absorption in Mg_2Ni alloys under mechanical processing conditions," *J. Mater. Sci.*, vol. 43, pp. 5193–5198, 2008.

[24] T. P. L. Pedersen, C. Liesch, C. Salinga, T. Eleftheriadis, H. Weis, and M. Wuttig, "Hydrogen-induced changes of mechanical stress and optical transmission in thin Pd films," *Thin Solid Films*, vol. 458, pp. 299–303, 2004.

[25] A. Taflove and M. E. Brodwin, "Numerical solution of steady-state electromagnetic scattering problems using the time-dependent Maxwell's equations," *IEEE Trans. Microw. Theory Tech.*, vol. MTT-23, no. 8, pp. 623–630, Aug. 1975.

[26] J. P. Verboncoeur, A. B. Langdon, and N. T. Gladd, "An object-oriented electromagnetic PIC code," *Comput. Phys. Commun.*, vol. 87, pp. 199–211, 1995.

[27] C. K. Birdsall and A. B. Langdon, *Plasma Physics via Computer Simulation*. New York: McGraw-Hill, 1985.

[28] B. Goplen, L. Ludeking, D. Smithe, and G. Warren, "User-configurable MAGIC for electromagnetic PIC simulation," *Comput. Phys. Commun.*, vol. 87, pp. 54–86, 1995.

[29] Y. Li, H.-W. Cheng, C.-C. Lin, and F.-M. Pan, "Field emission property of carbon nanotube field emitters in triode structure fabricated with anodic aluminum oxide templates," *Jpn. J. Appl. Phys.*, vol. 47, pp. 3282–3286, 2008.

[30] Y. Li, H.-M. Chou, J.-W. Lee, and B.-S. Lee, "A three-dimensional simulation of electrostatic characteristics for carbon nanotube array field effect transistors," *Microelectron. Eng.*, vol. 81, no. 2–4, pp. 434–440, Aug. 2005.

[31] R. H. Fowler and L. W. Nordheim, "Electron emission in intense electric fields," *Proc. R. Soc. Lond. A*, vol. 119, no. 781, pp. 173–181, 1928.
[32] T. E. Stern, B. S. Gosling, and R. H. Fowler, "Further studies in the emission of electrons from cold metals," *Proc. R. Soc. Lond. A*, vol. 124, no. 795, pp. 699–723, 1929.
[33] H. B. Michaelson, "The work function of the elements and its periodicity," *J. Appl. Phys.*, vol. 48, pp. 4729–4733, 1977.
[34] R. Dus, R. Nowakowski, and E. Nowicka, "Chemical and structural components of work function changes in the process of palladium hydride formation within thin Pd film," *J. Alloys Compound*, vol. 404–406, pp. 284–287, 2005.
[35] S. Yamamoto, "Fundamental physics of vacuum electron sources," *Rep. Prog. Phys.*, vol. 69, no. 1, pp. 181–232, 2006.

Yiming Li (M'02) received the B.S. degree in applied mathematics and electronics engineering, the M.S. degree in applied mathematics, and the Ph.D. degree in electronics from the National Chiao Tung University (NCTU), Hsinchu, Taiwan, in 1996, 1998, and 2001, respectively.

In 2001, he joined the National Nano Device Laboratories (NDL), Hsinchu, as an Associate Researcher, where he was the Director of the Departments of Nanodevice and Computational Nanoelectronics from 2003 to 2005 and is currently the Deputy Director General. In 2001, he also joined the Microelectronics and Information Systems Research Center (MISRC), National Chiao Tung University (NCTU), as an Assistant Professor, where he was an Associate Professor from 2003 to 2005, has been an Associate Professor with the Department of Communication Engineering since Fall 2004, has been a Full Professor with the Department of Electrical Engineering since Fall 2008, is currently the Deputy Director of the Modeling and Simulation Center, conducts the Parallel and Scientific Computing Laboratory, and has been engaged in the field of computational science and engineering, particularly in modeling, simulation, and optimization of nanoelectronics and very large scale integration (VLSI) circuits. In Fall 2002, he was a Visiting Assistant Professor with the Department of Electrical and Computer Engineering, University of Massachusetts at Amherst. From 2003 to 2004, he was a Research Consultant of the System on a Chip (SOC) Technology Center, Industrial Technology Research Institute (ITRI), Hsinchu. He has authored or coauthored more than 200 research papers published in international book chapters, journals, and conferences. He has been a reviewer, a guest associate editor, a guest editor, an associate editor, and an editor for many international journals. His current research interests include computational electronics and physics, physics of semiconductor nanostructures, device modeling, parameter extraction, and VLSI circuit simulation, development of technology computer-aided design (TCAD) and electronic CAD (ECAD) tools and SOC applications, bioinformatics and computational biology, and advanced numerical methods, parallel and scientific computing, optimization techniques, and computational intelligence.

Prof. Li is a member of the Phi Tau Phi, the Sigma Xi, the American Physical Society, the American Chemical Society, the Association for Computing Machinery, the Institute of Electronics, Information and Communication Engineers (IEICE), Japan, and the Society for Industrial and Applied Mathematics. He has organized and served on several international conferences and was an editor for the proceedings of international conferences. He has been a reviewer for the IEEE TRANSACTIONS ON NANOTECHNOLOGY, the IEEE TRANSACTIONS ON EVOLUTIONARY COMPUTATION, the IEEE TRANSACTIONS ON MICROWAVE THEORY AND TECHNIQUES, the IEEE TRANSACTIONS ON COMPUTER-AIDED DESIGN OF INTEGRATED CIRCUITS AND SYSTEMS, the IEEE ELECTRON DEVICE LETTERS, and the IEEE TRANSACTIONS ON ELECTRON DEVICES. He was the recipient of the 2002 Research Fellowship Award presented by the Pan Wen-Yuan Foundation, Taiwan, and the 2006 Outstanding Young Electrical Engineer Award from the Chinese Institute of Electrical Engineering, Taiwan. He is also included in *Who's Who in the World*.

Hui-Wen Cheng (S'08) received the B.S. degree in atmospheric sciences from the National Taiwan University, Taipei, Taiwan, in 2003. Under the supervision of Professor Yiming Li, she is currently working toward the Ph.D. degree at Parallel and Scientific Computing Laboratory, Institute of Communication Engineering, National Chiao Tung University, Hsinchu, Taiwan.

Her current research interests include numerical modeling and computer simulation of semiconductor nano-CMOS and photonic devices.

Ms. Cheng was the recipient of the Best Paper Award at the 2008 International Electron Devices and Materials Symposia, Taiwan.